Optical nanorod antennas as dispersive one-dimensional Fabry–Pérot resonators for surface plasmons

Ertugrul Cubukcu[1,2,a)] and Federico Capasso[2,a)]
[1]*NSF Nano-scale Science and Engineering Center (NSEC), 3112 Etcheverry Hall, University of California, Berkeley, California 94720, USA*
[2]*School of Engineering and Applied Sciences, Harvard University, 29 Oxford Street, Cambridge, Massachusetts 02138, USA*

(Received 9 July 2009; accepted 21 October 2009; published online 16 November 2009)

Resonant optical nanoantennas exhibit a different length scaling due to the surface plasmons compared to their radio frequency counterparts. In this letter, we address this difference by calculating the wavelength-dependent effective mode index n_{eff} for a cylindrical one-dimensional gold nanowire waveguide. Our results show that nanorod optical antennas act as dispersive and lossy Fabry–Pérot resonators for surface plasmons. © *2009 American Institute of Physics*. [doi:10.1063/1.3262947]

Optical antennas have been of great interest in the past several years for numerous applications relying on the large near-field enhancements they offer along with their ability to confine electromagnetic radiation to subwavelength dimensions.[1–5] Radio frequency (rf) antennas are used for transmitting and receiving radio signals and are impedance matched to electronic circuits.[6,7] On the contrary, their optical counterparts are of interest primarily for their localized surface plasmon (SP) resonances originating from the collective motion of the free electrons in metals.[8,9] The SP resonances of metallic nanoparticles can be utilized to bridge the size gap, for efficient optical excitation, between a diffraction-limited optical spot and a single fluorescent dye molecule.[10] In addition, the local density of photonic states is also modified in the proximity of a nanoantenna resulting in enhanced or quenched photoluminescence from a dipole emitter.[10,11]

In the rf range, electromagnetic properties of metals can be described by surface wave impedances since metals reflect rf waves almost perfectly.[8] However, for optical frequencies, the ratio of the metal's skin depth to the free space wavelength becomes significantly larger allowing for strongly confined SP modes with effective indices larger than that of the surrounding dielectric materials. Consequently, their dipole resonances do not appear at multiples of half the free space wavelength.[3,5,8,12] Here, we show that these resonances rather occur at integer multiples of half the effective wavelength of the SP mode corresponding to Fabry–Pérot modes of the nanoantenna resonator.

It has been experimentally shown that chemically synthesized silver nanowires act as resonators for SPs.[13] Gold nanowires similarly exhibit such behavior.[14] A typical Fabry–Pérot spectrum of a 5 μm gold nanowire calculated numerically using a commercial finite integration technique code (CST Microwave Studio) is shown in Fig. 1. The diameter of the nanowire was chosen as 40 nm and the nanowire ends are realistically rounded with a radius of curvature of 20 nm. The nearfield enhancement spectrum was calculated at one of the extremities of the nanowire that was illuminated by a plane wave. Its polarization was tilted 15° with respect to the nanowire axis in order to ensure that all the odd and even modes are excited in the nanowire.

For shorter nanowire lengths, we expect to have resonances that are spectrally farther apart in analogy to the larger mode spacing in a shorter Fabry–Pérot cavity. Figure 2 shows the nearfield spectrum for a 500 nm long nanorod antenna of 40 nm diameter with rounded ends. The three-dimensional antenna problem is simulated using the finite integration technique. In these simulations, for plane wave illumination with polarization along the nanorod only the odd antenna ($\lambda/2$ and $3\lambda/2$) modes are excited whereas for the 30°-tilted case, three dipolar resonances appear in the spectrum including the first even (λ) mode. This second resonance cannot be excited with a plane wave for normal incidence since this mode exhibits a charge distribution that has the same sign at different antenna ends. In other words, the overlap integral of this even mode and a plane wave polarized along the antenna axis is zero. However, by tilting the polarization with respect to the nanorod axis the radial polarization component of the SP mode can be driven allowing for finite coupling efficiency also into the second antenna resonance.

In conventional Fabry–Pérot resonators, the quality factor of the resonances is limited by the reflectivity of the end

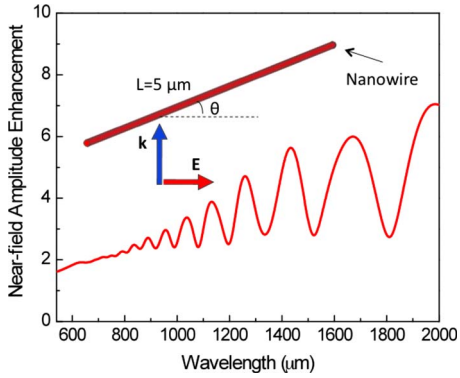

FIG. 1. (Color online) A typical Fabry–Pérot resonance spectrum calculated for a 5 μm long gold nanowire. The diameter of the nanowire is 40 nm. The angle θ between the plane wave polarization and the nanowire is 15°. Inset: The schematic of the gold nanowire excitation.

a)Authors to whom correspondence should be addressed. Electronic addresses: cubukcu@berkeley.edu and capasso@seas.harvard.edu.

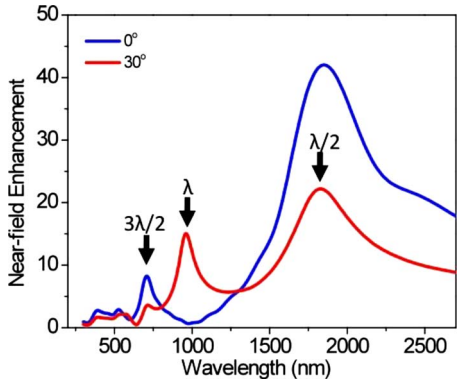

FIG. 2. (Color online) The calculated nearfield spectrum at the end of a 500 nm long gold nanorod for the normal and the 30°-tilted illuminations.

mirrors that make up the cavity. However, in this one-dimensional plasmonic version of the nanorod antennas, there are three different loss channels that affect the quality factor. The first one is the radiative damping due to oscillating charges in the gold nanorod. The second one is the material damping (Ohmic losses) due to absorption in gold at optical frequencies as the SPs propagate in the resonator. The third one is the reflection loss at the antenna ends yielding a low finesse cavity reminiscent of mirror losses in standard optical Fabry–Pérot cavities.

Another interesting feature of the optical nanorod antennas is their unusual length scaling due to the SP dispersion. For a typical dipole antenna of length L, the ratio L/λ is 0.5, 1, and 1.5, respectively, for the first three resonances (where λ is the free space wavelength) while in our case it is 0.27, 0.52, and 0.71. To address this discrepancy, we numerically calculated the effective one-dimensional mode refractive index for an infinitely long 40 nm diameter gold nanowire in air as a function of λ. The finite element method with experimental values for optical constants of gold[15] was used for calculating the modes. This method allows us to solve numerically for the waveguide modes of an infinitely long gold nanowire by only inputting the two-dimensional cross section of the nanowire in the transverse direction. We note that this is very similar to calculating the transverse modes of a cavity whereas the finite integration technique gives information about the longitudinal modes of a resonator.

Figure 3 shows the real and imaginary parts of the calculated wavelength dependent effective nanowire mode index n_{eff}. This TM like mode[16] is confined to the nanowire surface decaying exponentially away from the surface as shown in the inset of Fig. 3. A small longitudinal electric field component accompanies the large radially polarized component similar to two-dimensional SPs on a metal surface.[16] Below 1 μm wavelength where fields can penetrate significantly into the nanowire, the real part of n_{eff} increases rapidly. The mode also becomes very lossy as the wavelength approaches interband absorption in gold. By contrast, at infrared frequencies the mode index changes slowly with λ indicative of less field penetration into the metal. Consequently, fairly long propagation lengths can be achieved for one-dimensional SPs at longer wavelengths due to reduced material losses.

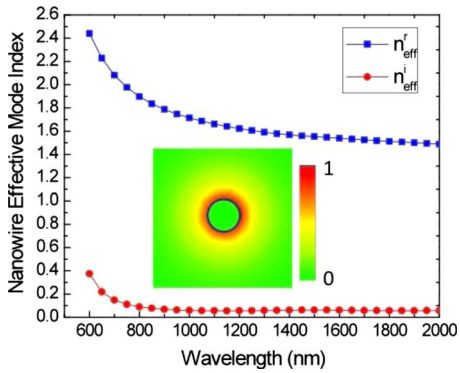

FIG. 3. (Color online) The real (blue squares) and the imaginary (red circles) parts of the effective nanowire mode refractive index as a function of wavelength. The nanowire diameter is chosen as 40 nm. The inset shows the mode profile for the radial component at 750 nm wavelength.

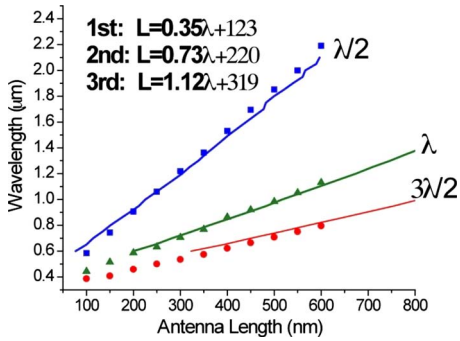

FIG. 4. (Color online) First three resonant antenna lengths as a function of illumination wavelength. The solid lines are calculated from Eq. (1) using effective mode refractive indices. The discrete points correspond to resonant wavelengths for fixed antenna lengths calculated with the finite integration technique. Parameters for linear fits to the mode index calculations are also listed for the first three resonances. These fit parameters are in nanometers for both L and λ.

Having calculated n_{eff}, we can write the antenna resonance condition as

$$m\frac{\lambda}{2n_{\text{eff}}(\lambda)} = L(\lambda) + 2\delta(\lambda), \tag{1}$$

where m is an integer denoting the order of the resonance and δ is a measure of how much the field penetrates in vacuum corresponding to the phase shift acquired upon reflection of the SP mode from the antenna ends. In other words, δ corresponds to the decay length of the displacement current in vacuum increasing the effective antenna length. We assume that δ is comparable to the $1/e$ decay length of the one-dimensional SP mode in the radial direction.

We calculate the resonant antenna length L in Eq. (1) for various wavelengths using values for δ and n_{eff} from the finite element method calculations. Figure 4 shows calculated values of L as a function of free space wavelength λ for the first three dipolar resonances. We compare these results with our rigorous resonance calculations. In the finite integration technique simulations, we set the length of the antenna and determine, by solving the full vector electromagnetic problem, the resonance wavelengths that give the maximum near-field enhancement at the antenna ends similar to the simulation results shown in Fig. 2(a). The calculated near field enhancement peaks are also plotted for various antenna lengths in Fig. 4 for comparison. There is good agreement between the two approaches. Our findings show linear dependence between the free space wavelength and the antenna length for the first three orders. By making fits to

mode calculation results, we determined linear equations that can be used to determine resonant antenna lengths for a given wavelength and a resonance order as shown in Fig. 4. These equations can be used as a guide for designing optical antennas.

Another widely used antenna design utilizes two nanorods separated by a nanometric gap.[4] In this case, similar scaling with the antenna arm length is expected, however the resonances will be redshifted from the single nanorod antenna resonances due to the nearfield coupling between the two arms of the antenna.

In summary, we show that nanorod optical antennas act as one-dimensional Fabry–Pérot resonators for SPs. We also address the different scaling of optical antennas compared to their radio frequency counterparts by incorporating the wavelength dependent SP mode index. These results will be useful for future optical antenna designs that are important for surface enhanced spectroscopies and light matter interaction on the nanometer scale.

We acknowledge support from the Air Force Office of Scientific Research Multidisciplinary University Research Initiative Program (AFOSR MURI on Plasmonics) and NSF NSEC under Award No. DMI-0327077.

[1]K. B. Crozier, A. Sundaramurthy, G. S. Kino, and C. F. Quate, J. Appl. Phys. **94**, 7950 (2003).
[2]P. J. Schuck, D. P. Fromm, A. Sundaramurthy, G. S. Kino, and W. E. Moerner, Phys. Rev. Lett. **94**, 017402 (2005).
[3]P. Muhlschlegel, H. J. Eisler, O. J. F. Martin, B. Hecht, and D. W. Pohl, Science **308**, 1607 (2005).
[4]E. Cubukcu, E. A. Kort, K. B. Crozier, and F. Capasso, Appl. Phys. Lett. **89**, 093120 (2006).
[5]E. Cubukcu, N. F. Yu, E. J. Smythe, L. Diehl, K. B. Crozier, and F. Capasso, IEEE J. Sel. Top. Quantum Electron. **14**, 1448 (2008).
[6]A. Alu and N. Engheta, Nat. Photonics **2**, 307 (2008).
[7]A. Alu and N. Engheta, Phys. Rev. Lett. **101**, 043901 (2008).
[8]L. Novotny, Phys. Rev. Lett. **98**, 266802 (2007).
[9]M. Danckwerts and L. Novotny, Phys. Rev. Lett. **98**, 026104 (2007).
[10]P. Anger, P. Bharadwaj, and L. Novotny, Phys. Rev. Lett. **96**, 113002 (2006).
[11]P. Bharadwaj, P. Anger, and L. Novotny, Nanotechnology **18**, 044017 (2007).
[12]G. Schider, J. R. Krenn, A. Hohenau, H. Ditlbacher, A. Leitner, F. R. Aussenegg, W. L. Schaich, I. Puscasu, B. Monacelli, and G. Boreman, Phys. Rev. B **68**, 155427 (2003).
[13]H. Ditlbacher, A. Hohenau, D. Wagner, U. Kreibig, M. Rogers, F. Hofer, F. R. Aussenegg, and J. R. Krenn, Phys. Rev. Lett. **95**, 257403 (2005).
[14]B. J. Wiley, D. I. Lipomi, J. M. Bao, F. Capasso, and G. M. Whitesides, Nano Lett. **8**, 3023 (2008).
[15]E. D. Palik, *Handbook of Optical Constants of Solids* (Academic, New York, 1985), Vol. 1.
[16]J. Takahara, S. Yamagishi, H. Taki, A. Morimoto, and T. Kobayashi, Opt. Lett. **22**, 475 (1997).